Characteristics of a Frictional Pressure Drop for a Cross-flow over the Horizontal Tube Banks in a Sodium-to-sodium Heat Exchanger with a Helical Tube Arrangement

Hyung Gyun Noh [a], Jaehyuk Eoh [b*], Dong Eok Kim [c], Moo Hwan Kim [a]

[a] *Division of Advanced Nuclear Engineering, POSTECH, Pohang*
[b] *Korea Atomic Energy Research Institute, Fast Reactor Development Div., 1045 Daedeok-daero, Daejeon*
[c] *Department of Precision Mechanical Engineering, Kyungpook National University, Sangju*
[*]*Corresponding author: jheoh@kaeri.re.kr*

1. Introduction

After the Fukushima nuclear power plant (NPP) accident, the enhancement of plant safety becomes one of the most significant concerns. To achieve this goal, The Korea Atomic Energy Research Institute (KAERI) has been developing the own sodium-cooled fast reactor (SFR) and proposed the creative design concept of the combined IHX-DHX unit, called CHX (Combined Heat eXchanger). Unlike the traditional decay heat removal concept with a parallel heat removal flow path with IHXs and DHXs, a new heat exchanger design concept of the CHX unit has been implemented in an innovative decay heat removal system in SFRs, which uses a simplified flow path from the hot sodium pool to the cold pool through a serialized coolant path passing the DHX and IHX as compared in Figure 1 [1].
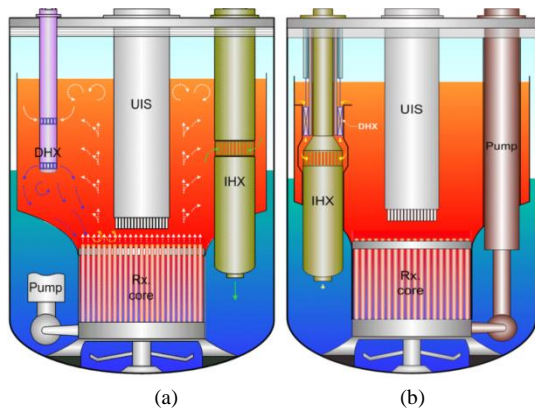
(a) Typical configuration of HXs inside the RV
(b) New design and configuration of the CHX unit
Fig. 1. Comparison of the heat exchangers configuration in the primary coolant system in SFR [1]

The combined IHX-DHX unit (CHX) is a shell-and-tube type counter-current flow heat exchanger with a helically-coiled tube arrangement. Figure 2 shows the general configuration of the CHX unit with the IHX coaxial pipe arrangement that located inside the reactor vessel. Total 4-row heat transfer tube bundle of the DHX surrounds the coaxial part of the IHX unit, and its lower end is vertically placed above the IHX inlet window nozzle. The annular-type sodium downcomer chamber surrounds the IHX coaxial pipe, and an annular-type hot sodium riser chamber surrounds it as well. From this design features, quadruple sodium chambers configure the segregated sodium flow paths of the DHX and IHX units.
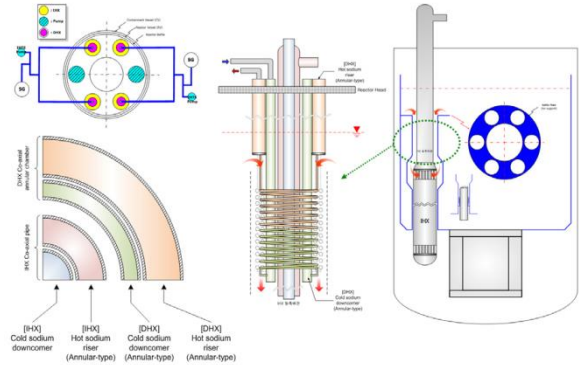

Fig. 2. Configuration of the CHX unit [2]

To this end, shell-side flow pattern of the CHX unit can be assumed to be a cross-flow over the horizontal tube banks. Each helical tube is configured with the inclined angle of approximately seven degrees with the horizontal direction crossing the flow.

The main objective of this study is to investigate the characteristics of the frictional pressure drop for a cross-flow over the horizontal tube banks in the shell-side of the CHX unit. To determine the pressure distributions on the shell-side of the CHX unit, numerical simulation using the commercial CFD package, ANSYS CFX 16.2, has been performed in the present study. The physical models of the pressure drop across a tube bank were described first complying with the shell-side CHX geometry. Quantities of the pressure drops were obtained from both the empirical formula and the CFD analysis in terms of operating conditions, such as the 100% steady-state and DHR (Decay Heat Removal) mode in SFRs. In the present study, the analysis results of pressure distributions were compared each other and the flow characteristics in a cross-flow regime like a shell-side CHX are discussed as well.

2. Models and verification method
2.1 Configuration of the combined IHX-DHX unit (CHX)

To investigate and verify the detailed characteristics of pressure distributions in a cross-flow sodium flow across the tube banks, the scaled-down model CHX unit was designed first on the prototype CHX unit that is potentially employed in a practical SFR design. To preserve general flow and heat transfer performance of the prototype CHX unit, the scaling design has been carefully made complying with the specified scaling method [3]. In the model CHX unit, the tube bundle of

the CHX unit consists of four rows and eleven columns as depicted in Figure 3. All tubes are sequently installed in a radial direction arrays with. Each helical coil array has a different radius from the center of the inner shell and has been installed with alternating directions for every other tube row.
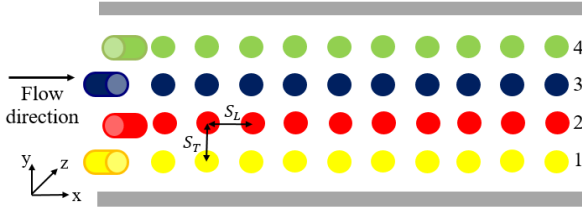

Fig. 3. Arrangement of tube banks in the shell-side CHX

The tube outer diameter is 27.2mm, and the ratios of transverse and logitudinal pitch are set to be 2.65 and 1.75, respectively. Volumetric hydraulic diameter defined by Gunter-shaw [4] is obtained to be 0.1334m. Other geometric details are described in Table.1.

Table.1. Specific design parameters of the model CHX unit [1]

CHX design parameters	Model CHX
Pitch to diameter ratio (P_T / P_L)	2.65 / 1.75
Tube OD/ID (mm)	27.2/23.9
Tube thickness (mm)	1.65
Volumetric hydraulic diameter (D_v, m)	0.1334
Tube bundle height (m)	0.524
The number of tubes (N_T / N_L)	4 / 11
Shroud inner OD/ outer ID (m)	0.728 / 1.332

2.2 Zukauskas model for frictional pressure drop

Zukauskas proposed empirical models for predicting the frictional pressure drop across the tube banks in a cross-flow regime [5]. The Reynolds number and the maximum velocity are defined as the following equations (1) and (2).

$$Re_Z = \frac{\rho V_{max} D}{\mu} \qquad (1)$$

$$V_{max} = \frac{S_T}{S_T - D} V \qquad (2)$$

Besides, the Zukauskas pressure drop model can also be expressed as equation (3).

$$\Delta P = N_L \chi f (\rho V_{mxx}^2 / 2) \qquad (3)$$

2.3 Gunter-Shaw model for frictional pressure drop

The Reynolds number of an inter-flow inside a tube bank can be defined by Gunter-Shaw as equation (4), and also suggested the empirical formula of pressure drop in a cross-flow over a bare tube bank as equation (5) [4].

$$Re_G = \frac{\rho V_{max} D_V}{\mu} \qquad (4)$$

$$\Delta P = \frac{f}{2} \frac{G^2 L}{\rho D_v} (\frac{\mu}{\mu_w})^{0.14} (\frac{D_V}{S_T})^{0.4} (\frac{S_L}{S_T})^{0.6} \qquad (5)$$

The half friction factor can be expressed as equations (6) and (7). The transition point from the laminar to turbulent flow is defined at a Reynolds number of approximately 200 in Gunter-Shaw correlation.

$$\frac{f}{2} = 90 \, Re^{-1} \text{ for Re} \leq 200 \qquad (6)$$

$$\frac{f}{2} = 0.96 \, Re^{-0.145} \text{ for Re} > 200 \qquad (7)$$

2.4 Numerical simulation for pressure drop calculation

Numerical simulations using the commercial CFD package, ANSYS CFX 16.2, were carried out for evaluating frictional pressure drop in a complicated flow path of the shell-side CHX unit. The CFD analyses were conducted at the 100% power operating condition as well as that of DHR mode. The 3-dimensional shape of the model CHX unit shown in Fig. 4 was implemented in the CFD analysis. The domains of the CFD analysis were largely divided into 3 parts, which are the shell-side flow region, tube-side flow region, and the structure part of the CHX unit.
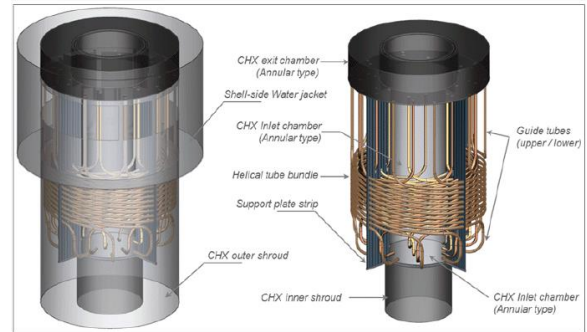

Fig. 4. 3-dimensinal shape of the model CHX unit

The total number of calculation nodes and elements for each CFD simulation are approximately 41,000,000 and 141,000,000, respectively. The tetra and prism grid were used as shown in Fig. 5. The inlet and outlet regions are expanded for convergence.
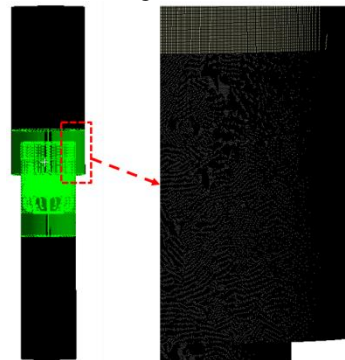

Fig. 5. Numerical domain in shell-side of model CHX

For the boundary conditions, the inlet flow rates for both cases of the DHR mode and 100% operating condition were set to be 9.45 kg/s and 523 kg/s, respectively. The same temperature condition of 510℃ has been applied at the inlet, and zero Pa was also applied as the outlet boundary condition. In regard to the

numerical convergence criteria, the residuals of energy and momentum were commonly set to be less than 0.001. All flux imbalances converge criteria were set within 0.1% as well.

2.5 Results and discussion

The frictional pressure drop of the shell-side CHX unit was determined by using the CFD simulation at the DHR mode and 100% operating condition. The CFD analysis results of overall pressure distributions for both cases were respectively shown in Fig. 6. The pressure drops between inlet and outlet of the helical tube bank are approximately 0.165 Pa and 288.179 Pa at the DHR mode and 100% operating condition, respectively. It was quantitatively observed that the pressure drop at the DHR mode is significantly small enough to ignore. On the other hand, at 100% operating condition, it was observed to be considerably larger than that of the DHR mode. The main reason for the large amount of pressure drop at the 100% operating condition is due to the high fluid velocity.

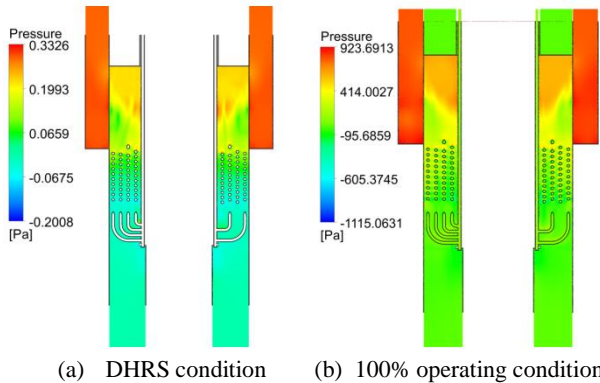(a)   DHRS condition   (b) 100% operating condition
Fig. 6. Pressure distribution in vertical section of model CHX

For both the DHR mode and 100% operating conditions, the values of the frictional pressure drops calculated by the empirical formulas suggested by Gunter-shaw and Zukauskas were compared with the analysis results from the CFD analysis. All comparison results are shown in Fig. 7 at a glance. The x-axis means the Reynolds numbers based on the Gunter-Shaw correlation. It was observed that the frictional pressure drops from the Zukauskas correlation overestimates those of the Gunter-Shaw at the range that Re_G is larger than 15,000.
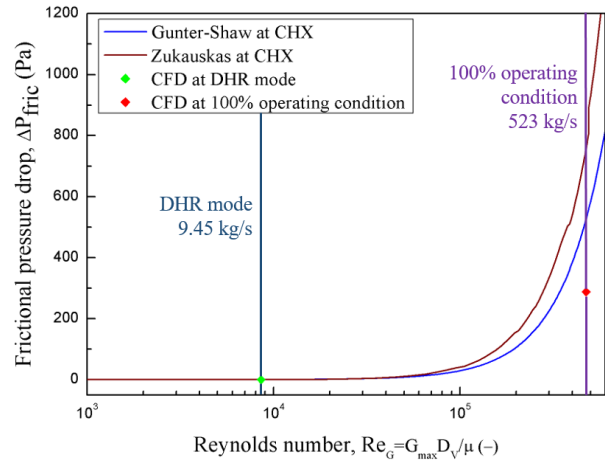

Fig. 7. Frictional pressure drops in terms of Reynolds numbers based on the Gunter-Shaw correlation

Due to the extremely small flow rate at the DHR mode, it was estimated that the discrepancies between the results of the CFD analysis and the empirical formulas, such as the Gunter-Shaw and Zukauskas correlations, are only 0.135 Pa and 0.110 Pa, respectively. Under the 100% operating condition, the discrepancy between the CFD analysis result and the Zukauskas correlation was estimated to be 61.86%, which is larger than those of the Gunter-Shaw correlation of 45.19%. To this end, these correlations do not well predict the CFD result at the 100% operating condition. Because it is unpredictable with existing correlations, it is experimentally necessary to develop empirical correlations that can predict the pressure drop in CHX of new concept.

3. Conclusions

The frictional pressure drops on the shell-side of the model CHX unit were investigated by using the commercial CFD package, ANSYS CFX 16.2 and conventional empirical formulas for the specific geometries. The frictional pressure drop models for the tube bank in cross-flow regime were assessed by comparing with the CFD analysis results for the actual CHX unit. A higher pressure drops were estimated at the 100% operating condition owing to the high fluid velocity in the shell-side CHX unit. It was found that the empirical correlations of the Gunter-Shaw and the Zukauskas for predicting the frictional pressure drops of the tube bank in a cross-flow regime do not show reasonable agreement with the CFD analysis results of the CHX unit. For a practical implementation of the innovative CHX design concept to the real sodium-cooled fast reactor, the frictional pressure drop models of the shell-side CHX unit should be experimentally verified in the future works.

Nomenclature

P_T: Transverse pitch to diameter ratio
P_L: Longitudinal pitch to diameter ratio
S_T: Transverse pitch (m)
S_L: Longitudinal pitch (m)
D: Tube outer diameter
D_V: Volumetric hydraulic diameter (m)
N_T: The number of tubes located in normal to flow direction
N_L: The number of tubes located in flow direction
Re_Z: Reynolds number based on Zukauskas correlation
Re_G: Reynolds number based on Gunter-Shaw correlation
V_{max}: maximum flow velocity (m/s)
ΔP: Frictional pressure drop (Pa)
μ: Absolute viscosity at average main stream temperature
μ_w: Absolute viscosity at surface wall temperature

REFERENCES

[1] J. H. Eoh et al., "Test Requirements for the Integral Effect Test to Simulate a Sodium-cooled Fast Reactor", KAERI/TR-4424/2011, Korea Atomic Energy Research Institute, 2011.
[2] J. H. Eoh et al., "Development of a Combined Heat Exchanger Design Concept for an SFR Decay Heat Removal System", KAERI/RR-3762/2015, Korea Atomic Energy Research Institute, 2015.
[3] J. H. Eoh et al., "Sodium Thermal-Hydraulic Test Program for Design Validation of Prototype Gen-IV Sodium-cooled Fast Reactor", International Congress on Advances in Nuclear Power Plants, Charlotte, 2018.
[4] A. Y. Gunter, W. A. Shaw, "A General correlation of friction factors for various types of surfaces in crossflow", Transactions of the A.S.M.E, Vol.67, No8, 1945.
[5] A. Zukauskas, "Heat transfer from tubes in cross flow", in: J.P. Hartnett, T.F. Irvine Jr. (Eds.), Adv. Heat Transfer, vol. 8Academic Press, New York, 1972.
[6] J. H. Eoh et al., Development of a Combined Heat Exchanger Design Concept for an SFR Decay Heat Removal System, Korea Nuclear Society, Gyeongju, 2012.
[7] J. H. Eoh et al., Evaluation of the Structure Design Concept of a Combined Heat Exchanger for Decay Heat Removal System in a Sodium-cooled Fast Reactor, Korea Nuclear Society, Gwangju, 2013.
[8] H. C. Kang, J. H. Eoh, J. E. Cha and S. O. Kim, Numerical study on pressure drop and heat transfer for designing sodium-to-air heat exchanger tube banks on advanced sodium-cooled fast reactor, Nuclear Engineering and Design, Vol.254, p.5-15, 2013.